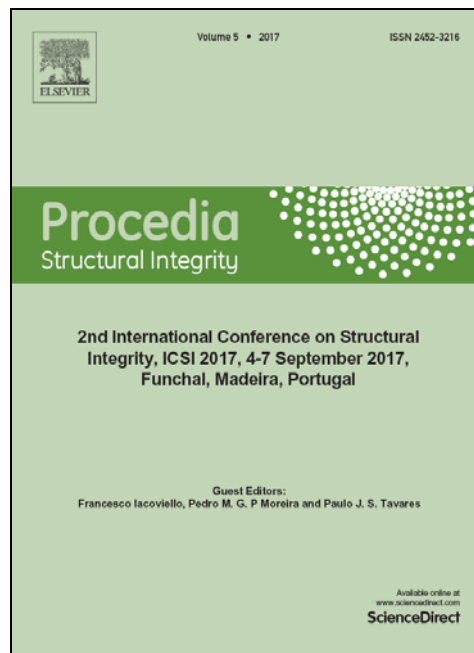Université de Mons
Faculté Polytechnique – Service de Mécanique Rationnelle, Dynamique et Vibrations
31, Bld Dolez - B-7000 MONS (Belgique)
065/37 42 15 – georges.kouroussis@umons.ac.be

L. Ben Fekih, O. Verlinden, C. De Fruytier, G. Kouroussis, Novel test prototype for the determination of mode I fracture parameters: application to adhesively bonded electronics, *Procedia Structural Integrity*, 5: 5–12, 2017.

2nd International Conference on Structural Integrity, ICSI 2017, 4-7 September 2017, Funchal, Madeira, Portugal

Novel test prototype for the determination of mode I fracture parameters: application to adhesively bonded electronics.

Lassaad Ben Fekih[a]*, Olivier Verlinden[a], Christophe De Fruytier[b], Georges Kouroussis[a]

[a]University of Mons, 20 Place du Parc, 7000 Mons, Belgium
[b]Thales Alenia Space, Rue Chapelle Beaussart, 6032 Mont-Sur-Marchienne, Belgium

Abstract

Structural adhesives are commonly used in space electronics particularly for bonding ceramic quad flat packages to printed circuit boards (PCB). In such application, adhesive joints are subjected to high loads due to the PCB bending under severe acceleration of the launch. It is thus mandatory to figure out the adhesive mechanical resistance in order to achieve a safe design. The present paper is concerned with the determination of the cohesive properties of an aerospace adhesive in tensile fracture mode. For this purpose, a novel test prototype consisting of a ceramic component adhesively bonded to a PCB plate is designed and tested subsequently in quasi-static loading. In parallel, a finite element (FE) model of the assembly is developed using ABAQUS software. The adhesive joint is modelled by user-defined cohesive elements. The latter are implemented using a FORTRAN user subroutine (UEL) capable of simulating the geometrical and material nonlinearities of the adhesive. A good agreement is obtained between experimental and numerical results after updating. This finding permitted to successfully find out the cohesive parameters of the tested adhesive.

Keywords: Fracture analysis, numerical modelling

* Corresponding author. Tel.: +32 65 37 42 16; fax: +32 65 37 41 83.
  E-mail address: lassaad.benfekih@umons.ac.be

Nomenclature

E_a, ν_a, G_a, h_a	Young's modulus, Poisson ratio, shear modulus, thickness of the adhesive
G_{IC}	critical mode I strain-energy release rate, or fracture toughness
G_C	total critical strain-energy release rate
K_i	stiffness for mode i
Δ_i	displacement jump for mode i
Δ_E	equivalent displacement jump
$\Delta_{0,i}$	damage onset displacement jump for mode i
$\sigma_{0,i}$	maximum cohesive stress for mode i
Δ_0	equivalent displacement jump at damage onset
Δ_F	equivalent failure displacement jump
D^0	undamaged stiffness tensor
D	interface stiffness tensor
d	damage variable
δ_{ij}	Kronecker delta

1. Introduction

Space electronic boards, part of the payload, are subjected during the launch phase to high levels of acceleration. Face to these environmental conditions, the maintain of a given electronic component to the board depends on its dimensions, weight and location on the printed circuit board (PCB). Most vulnerable components, i.e., large and heavy packages can fail under the bending response of the PCB. Because high stress is transmitted from the board to the attachment joints of the component, the use of structural adhesives may be necessary: either to solely maintain the electronic component, or to be used in conjunction with solder joints as consolidation. Ben Fekih et al. (2015b) detailed common adhesive joint geometries used in space electronic boards. Due to the high cost of space missions, a special care should be paid to the design of adhesive joints. To do so, a substantial task consists in characterizing these joints for static, dynamic and fatigue loads. The scope of this study concerns the determination of the fracture resistance of adhesive joints used to maintain ceramic quad flat packages on PCB under mode I tensile loading conditions. ISO-25217 (2009) defined standardized specimens for mode I adhesive fracture testing consisting of double cantilever beam (DCB) and tapered DCB (refer to Fig. 2). The determination of critical strain-energy release rate, referred to as toughness energy, within this standard relies on agreed analytical expressions. The latter are valid only under limited deflections and for quasi-static loading with no significant dynamic effects. Moreover, the mechanical behavior of the PCB, a laminate epoxy/glass composite, is nonlinear elastic. This differs from the behavior of common used substrate materials such as aluminum and titanium alloys which is linear. Hence, the first reported condition may readily be violated. On the one hand, the current case study consists of a tri-material assembly within PCB-adhesive and ceramic-adhesive interfaces. On the other hand, standard prototypes make use of the same material for both substrates which may not replicate reliably the actual adhesion in ceramic electronic assemblies. Another aspect to meet is related to load conditions: the delamination of the bonded assembly is expected to result from PCB bending only, i.e., without load applied to the ceramic component. Meanwhile, both substrates are loaded in standard test prototypes. The use of a PCB as substrate is of practical interest since it permits to report the state of the adhesive failure in function of the PCB deflection. In so doing, some empirical design rules of PCB boards based on PCB warpage could be validated. More insight about this topic is reported in Ben Fekih et al. (2015a). Note that few studies concentrated on the use of flexible substrates, e.g., Hasegawa et al. (2015) have retained the basic geometry of standard prototypes but rather used flexible reinforced laminate composite for substrates standard test geometries. Another drawback of classical fracture prototypes is the requirement of an initial pre-crack which may not necessarily be produced in practice. By

discarding the adhesive pre-crack, the preparation of the bonded assembly could be simpler and the discussion about the length of the crack tip may be fairly avoided. Any fracture test system should be provided with its corresponding analytical or numerical model. This invokes modelling the adhesive layer which may be done in different ways: the continuum mechanics approach is simple to implement, however, it suffers from mesh convergence. Ben Fekih et al. (2015a) have demonstrated that mesh refinement could not solve such issue due to the presence of singularities across the adhesive-substrate interface. The fracture approach supports the notion of singularities as it characterizes the adhesive joint resistance by a coefficient of stress singularity, mostly determined analytically, and a stress intensity factor possibly obtained by fitting against finite element results. More about this approach, could be read in Ben Fekih et al. (2016a). A more engineering approach consists in cohesive zone modelling (CZM): it is simple to implement, tolerates coarse adhesive mesh and remediates the problem of corner and edge singularities (refer to Da Silva et al. (2008)). Fernandes et al. (2017) considered that CZM approach is the best candidate to model the adhesive behavior. In fact, it takes into account the plasticization, or resistance, notably of ductile adhesives, after the onset of debonding. Chandra et al. (2002) established a comprehensive literature survey of shapes of cohesive laws (triangular, trapezoidal and linear-exponential). According to Fernandes et al. (2017) the triangular law offers an overall acceptable fit of the adhesive behavior.

In this paper, the theoretical background of CZM approach is first introduced. An ad-hoc novel prototype dedicated to the test of adhesively bonded ceramic electronic components is described. Next, a numerical approach based on CZM is employed to figure out the fracture toughness and the strength of the adhesive in tension through fit against experimental load-displacement curves.

2. Cohesive zone modelling approach: theoretical background

The adhesive mechanical behavior is modelled by a CZM approach. A triangular (bilinear) traction-separation law $(\Delta_i - \sigma_i)$ permits to express the stress component σ_i in function of the correspondent relative displacement of the two substrates, Δ_i. The index i takes one of the letters (N,T,S) which denote mode I normal opening, mode II sliding shear, and mode III scissoring shear, respectively. As reported in Balzani et al. (2012) these modes correspond to the three possible failure mechanisms in an adhesive joint. (N,T,S) can be confounded with (I,II,III) letters. All these definitions are incorporated into one analytical formulation of the bilinear cohesive law that is

$$\sigma_i^k = (1-d^k)D_{ij}^0\Delta_j^k - d^k D_{ij}^0 \delta_{Nj}\left\langle -\Delta_N^k \right\rangle \text{ with } i,j = (T,S,N) \tag{1}$$

where $\langle x \rangle = \frac{1}{2}(x+|x|)$ is the MacAuley bracket which inhibits any stiffness from change when interface surfaces are inter-penetrating. d^k is a damage variable defined afterwards. $\underline{\underline{D}}^0$ is the undamaged stiffness tensor expressed in terms of the adhesive joint mechanical and geometric properties given by

$$\underline{\underline{D}}^0 = \begin{bmatrix} K_T & 0 & 0 \\ 0 & K_S & 0 \\ 0 & 0 & K_N \end{bmatrix} \text{ where } K_N = \frac{E_a^{eff}}{h_a} \text{ with } E_a^{eff} = \frac{E_a(1-\nu_a)}{1-2\nu_a^2-\nu_a} \text{ and } K_S = K_T = \frac{G_a}{h_a} \tag{2}$$

where E_a, ν_a, G_a, h_a are Young's modulus, Poisson ratio, shear modulus and thickness of the adhesive, respectively. Ben Fekih et al. (2016b) have shown that the adhesive joint can be modelled by exact stiffness terms being reported in Eq. (2). The practical implementation of the bilinear traction-separation law starts with the calculus of damage onset displacement jump for each fracture mode, $\Delta_{0,i}$, when a mixed-mode failure is expected.

$$\Delta_{0,N} = \sigma_{0,N} / K_N, \ \Delta_{0,S} = \sigma_{0,S} / K_S \text{ and } \Delta_{0,T} = \sigma_{0,T} / K_T \tag{3}$$

The displacement jumps at an increment, k, are evaluated using stiffness values of the previous increment $k-1$. The second norm of the displacement jump vector, referred to as effective displacement jump, is given by

$$\Delta_E^k = \sqrt{\left(\Delta_N^k\right)^2 + \left(\Delta_S^k\right)^2 + \left(\Delta_T^k\right)^2} \tag{4}$$

The traction separation law encompasses damage initiation and propagation criteria. In mode I loading, the damage is initiated when the simulated displacement jump, Δ_N^k, becomes greater than the onset displacement jump of mode I,

$\Delta_{0,N}$. As shown on Fig. 1, the area under $(\Delta_I - \sigma_I)$ curve represents the critical energy-release rate of mode I which is given by

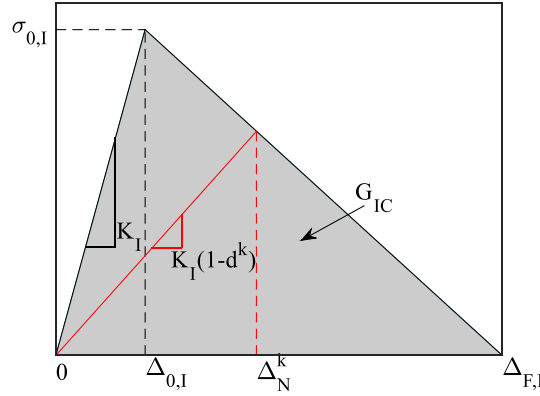$$G_{IC} = \frac{1}{2}\Delta_{F,I}\sigma_{0,I} \tag{5}$$

Fig 1. Bilinear cohesive law (mode I)

When being restricted to mode I the following relations are satisfied:

$$G_C = G_{IC}, \Delta_0 = \Delta_{0,I}, \Delta_F = \Delta_{F,I} \tag{6}$$

Based on equations (5) and (6), the final displacement whereby the cumulated cohesive energy reaches the critical value and complete decohesion occurs, is obtained by

$$\Delta_{F,I} = 2G_{IC}/\sigma_{0,I} . \tag{7}$$

A damage propagation criterion is required to model the stiffness degradation of the adhesive joint due to its softening. A damage variable, d^k, is defined to account for the damage progression at each increment, k, following

$$d^k = \min\left(1, \frac{\Delta_F(R^k - \Delta_0)}{R^k(\Delta_F - \Delta_0)}\right) \tag{8}$$

where $R^k = \max\left(\Delta_E^k, \frac{\Delta_0\Delta_F}{\Delta_F - d^{k-1}(\Delta_F - \Delta_0)}\right)$. $\tag{9}$

Thereby the initial stiffness tensor can be updated at each iteration as follows

$$\underline{\underline{D}}^k = (1 - d^k)\underline{\underline{D}}^0 \tag{10}$$

3. Experimental mode I fracturing of the adhesive assembly

The test assembly consists of a pure alumina ceramic component of dimensions 20x20x10 mm³ adhesively bonded from its beneath surface to a PCB of dimensions 120x20x1.85 mm³ using an aerospace epoxy adhesive, Loctite Ablestik 8-2 known as Tra-bond 8-2. The adhesive thickness is of 0.1 mm. Its uniformness is controlled using special calibrated spherical balls. The adhesive was cured at 75°C during 4 hours. The assembly is connected from its end to a rigid aluminum bar via a hinge joint. The second end of the intermediate bar is connected to a 5 kN load cell via a cardan joint. The load direction responsible for the adhesive joint opening in tension is depicted on Fig. 2. The length of the intermediate bar is chosen so as to maximally alleviate the angular deviation about the vertical N-axis. The objective is to obtain delamination of the assembly under the effect of PCB bending only and by preventing tension along T-axis (see Fig. 2). By so doing, a PCB deflection of 50 mm and an arm length of 130 mm yields an angular deviation of ±6° only. According to Karak et al. (2011), quasi-static testing should span the interval of load rates where the adhesive critical release rate energy positively deviates by less than 5 % from 0.1mm/min reference load

rate. ISO 25217 recommends 1 mm/min to 5 mm/min for joints prepared using fiber-composite substrates. Based upon these recommendations, a crosshead motion of 1 mm/min is applied by an INSTRON 4505 testing frame.
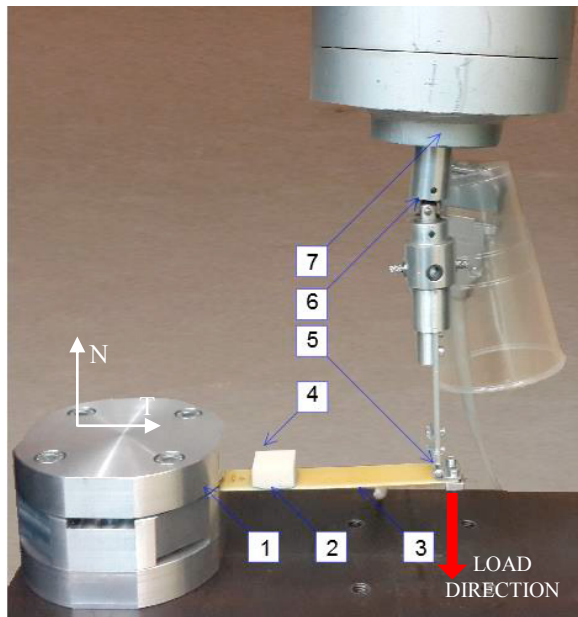
1. Rigid support—2. Adhesive joint—3. PCB—4. Ceramic component
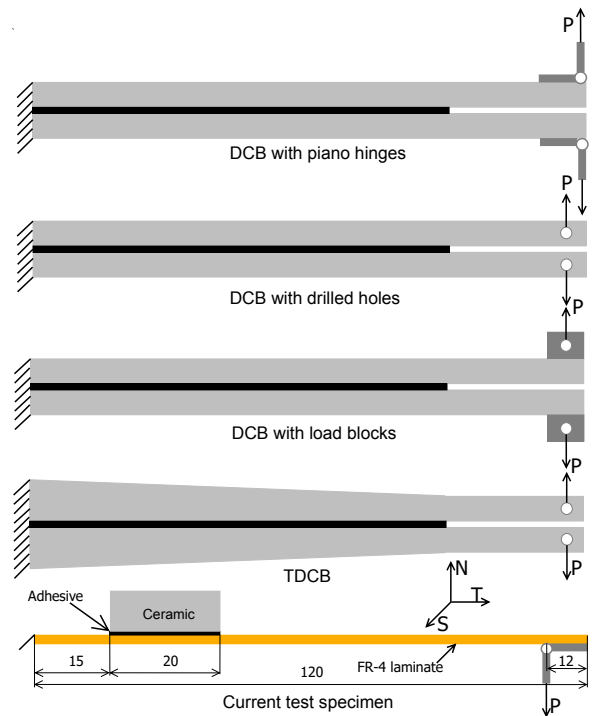5. Hinge joint—6. Cardan joint—7. Load cell

Fig. 2. Test Setup for mode I fracturing.

The damage is interfacial and is observed along the adhesive/PCB interface. With reference to Fig. 3, the experimental opening from the clamped side of the specimen is of 8.61 mm and of 6.63 mm from the loaded side.
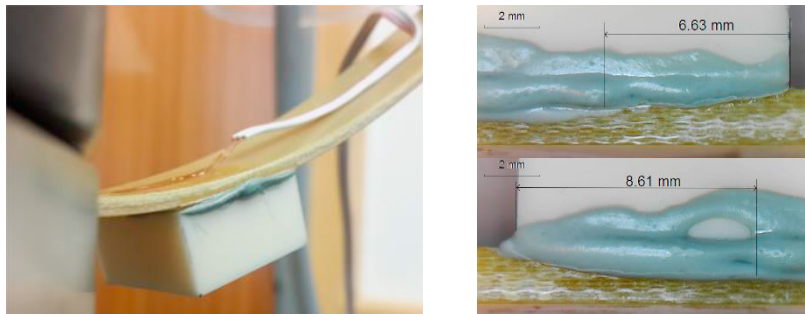

Fig. 3. Experimental determination of the debonding lengths.

4. Finite element model

The finite element (FE) model of the test prototype is developed under the commercial FE software ABAQUS. The PCB and the ceramic component are meshed using shell and structural quadratic elements, respectively (refer to Table 1). Alvarez et al. (2014) recommended mesh of the substrates with quadratic elements since their superiority in mesh-size dependence. Hinge and Cardan joints are included from the connectors library of ABAQUS. The PCB is expected

to reach large deflections in order to reach the maximum debonding of the assembly. Therefore, it is seen mandatory to account for the geometric nonlinearity. Non-linear elastic calculations can be activated through NLGEOM option of ABAQUS. Unfortunately, this feature does not support built-in cohesive elements. To bypass this drawback, a user-defined cohesive element is implemented via a UEL Fortran subroutine coupled subsequently to ABAQUS/Standard solver. The cohesive element is three-dimensional 8-node quadrilateral of four integration points. The adhesive joint is meshed by one layer of zero-thickness user-defined cohesive elements. An element size of 1 mm is seen satisfactory to yield stable integration scheme and acceptable computation time. According to Alvarez et al. (2014) the use of an element size larger than 2 mm remains problematic regarding the stability of the solution. Tie interactions ensured the link between nodes of the substrates and ones of the adhesive. An initial step time increment of 0.02 s is chosen. A three dimensional model is developed since it is intended to use the same UEL subroutine for mixed-mode loading later in this project. Besides this choice permits to avoid make stress/stain plane assumptions associated with two dimensional models.

5. Calibration of the PCB and the adhesive mechanical properties

5.1. Mechanical properties of the PCB

Preliminary bending tests were undertaken on two PCB-only cantilever specimens. An iterative calibration strategy is operated in order to obtain the best matching between experimental and numerical load-displacement curves. It appears from Fig. 4 an excellent agreement for Young's modulus of the PCB of 17.75 GPa. The obtained result permitted, also, to verify that no substrate plasticization had occurred at least until 45 mm of PCB deflection. Eventually, it asserts that the connectors are correctly placed into the FE model.

Table 1. Listing of the FE model components.

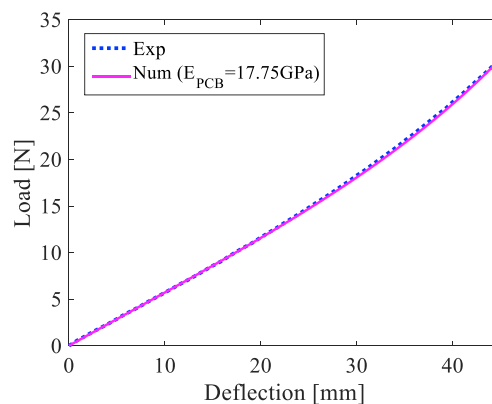| Components	Material	Type of element	Young's modulus (GPa)	Poisson ratio
PCB	Epoxy/ glass fiber laminate	S4	17.75	0.34
Ceramic	Pure Alumina (99% Al2O3)	C3D8	301	
Adhesive	Loctite Ablestik 8-2	User-defined	3.85*	0.43*
*mechanical properties determined through a dynamic mechanical analysis by Ben Fekih et al. (2016b).				

Fig. 4. Calibration of the numerical model of PCB only.

5.2. Cohesive properties of the adhesive

A parametric study is performed where the fracture toughness is varied while keeping the cohesive onset stress constant, Fig. 5(a), and vice versa, Fig. 5(b). It can be remarked that the model is very sensitive to G_{IC} and σ_0 change. The domain of work is comprised between the load-displacement curve of a bare PCB and the one of a rigidly bonded assembly (dashed lines). The shape of the load-displacement curve of the bonded assembly is mainly affected by the fracture toughness of the adhesive. This parameter is responsible for the region of high loads. It is worth noticing that during experiments the component was not entirely debonded. Consequently, a relevant fracture toughness should not conduct by simulation to a total debond. By comparison against experimental results, it is seen that a value of G_{IC} comprised between 0.15 and 0.175 kJ/m² could be fairly adopted. The cohesive onset stress controls the slope of the load-displacement curve for initial load levels. The maximum cohesive stress could be estimated at 10 MPa. According to Alvarez et al. (2014), the cohesive stress σ_0 obtained from mode I testing can be interpreted as uniaxial yield stress of the adhesive by assuming that the initiation is due to plastic yielding of the adhesive. These properties could be better refined by an iterative optimization procedure. The designer could anyway use lower bounds which increase the degree of security when applying this result.
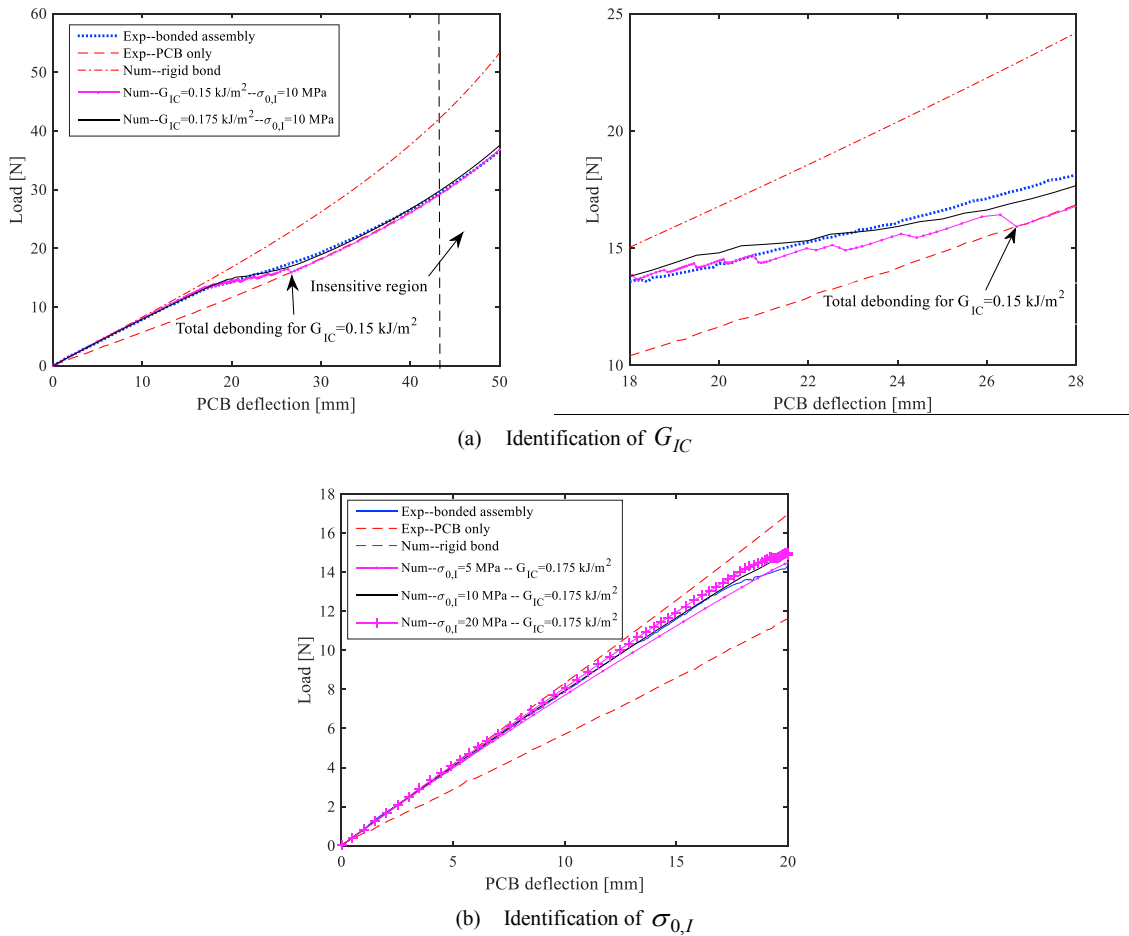

(a)　　Identification of G_{IC}

(b)　　Identification of $\sigma_{0,I}$

Fig. 5. Fit of the adhesive cohesive properties.

6. Conclusion

A novel prototype is designed for the purpose of characterizing adhesive joint in mode I fracture. The latter is devoted to structural adhesives used in bond of electronic ceramic components to space circuit boards which are subjected to high bending stress. In this work, a numerical finite element model has been developed using CZM bilinear law to simulate of the adhesive joint behavior. A combined experimental/numerical approach evaluated with success the tensile fracture toughness and yield strength of the tested aerospace adhesive. Simulation results, in good agreement with test results, demonstrated the feasibility of the designed test prototype. To confirm this proof-of-concept, the present prototype should be tested for a wider selection of adhesives.

Acknowledgements

References

Balzani, C., Wagner, W., Wilckens, D., Degenhardt., R., Busing., S., Reimerdes., H.-G., Adhesive joints in composite laminates—A combined numerical experimental estimate of critical energy release rates, International Journal of Adhesion & Adhesives 32(2012),23-38.

Ben Fekih, L., Verlinden, O., De Fruytier, Ch., Kouroussis, G., Novel stress-based criterion for the design of adhesive-bonded space electronics, Proceedings of the 4th European Conference on Spacecraft Structures, Materials and Environmental Testing (ECSSMET), Toulouse, France (2016a).

Ben Fekih, L., Verlinden, O., De Fruytier, Ch., Kouroussis, G., On the non-linear dynamic properties of Trabond 8.2 structural adhesive. Proceedings of the 23rd International Congress on Sound and Vibration (ICSV23), Athens, Greece, (2016b).

Ben Fekih, L., Kouroussis G., Verlinden O., Verification of empirical warp-based design criteria of space electronic boards, Microelectronics Reliability, 55, 12B, 2786-2792 (2015a).

Ben Fekih, L., Kouroussis, G., De Fruytier, Ch., Verlinden, O., Robustness evaluation of adhesively bonded ceramic quad flat chips for space applications, Vibration Engineering and Technology of Machinery, Springer International Publishing, (2015b) 547-557.

Chandra, N., Li, H., Shet, C., Ghonem, H., Some issues in the application of cohesive zone models for metal–ceramic interfaces, International Journal of Solids and Structures, 39(10) (2002), 2827-2855.

Da Silva, L.F.M., Öchsner, A., Modeling of adhesively bonded joints, Springer Berlin Heidelberg, (2008).

Di Leo, C.V., Luk-Cyr, J., Liu, H., Loeffel, K., Al-Athel, K., Anand, L. A new methodology for characterizing traction-separation relations for interfacial delamination of thermal barrier coatings, Acta Materialia, 71, (2014), 306-318.

Fernandes, R.L., Campilho, R.G.S.G., Testing different cohesive law shapes to predict damage growth in bonded joints loaded in pure tension, The Journal of Adhesion, 93 (2017), 57-76.

ISO-25217, Adhesives — Determination of the mode 1 adhesive fracture energy of structural adhesive joints using double cantilever beam and tapered double cantilever beam specimens, (2009).

Hasegawa, K., Crocombe, A.D., Coppuck, F., Jewel, D., Maher, S., Characterising bonded joints with a thick and flexible adhesive layer–Part 1: Fracture testing and behaviour. International Journal of Adhesion and Adhesives, 63 (2015), 124-131.

Karac, A., Blackman, B.R.K., Cooper, V., Kinloch, A.J., Rodriguez Sanchez, S., Teo, W.S., Ivankovic , A., Modelling the fracture behaviour of adhesively-bonded joints as a function of test rate, 78 (6) (2011), 973-989.

Turon, A., Camanho, P.P., Costa, J., Renart, J., Accurate simulation of delamination growth under mixed-mode loading using cohesive elements: Definition of interlaminar strengths and elastic stiffness. Composite structures, 92 (2010), 1857-1864.